Contents lists available at ScienceDirect

# Journal of Hazardous Materials

# Detection of dimethyl methylphosphonate by thin water film confined surface-enhanced Raman scattering method

Jingjing Wang [a], Guotao Duan [a,*], Guangqiang Liu [a], Yue Li [a], Zhengxing Chen [b], Lei Xu [c], Weiping Cai [a,*]

[a] Key Lab of Materials Physics, Anhui Key Lab of Nanomaterials and Nanotechnology, Institute of Solid State Physics, Chinese Academy of Sciences, Hefei 230031, PR China
[b] The Third Department, Institute of Chemical Defence, Beijing 120205, PR China
[c] East China Research Institute of Electronic Engineering, Hefei 230088, PR China

## HIGHLIGHTS

- A thin water film confined surface-enhanced Raman scattering method is proposed.
- DMMP molecules are successfully detected by our proposed enhanced Raman method.
- Surface superhydrophobicity and high laser power benefit the detection of DMMP.

## GRAPHICAL ABSTRACT
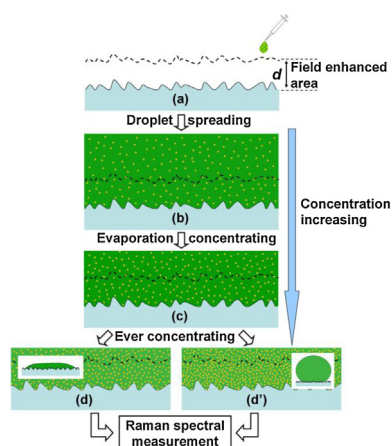


## ARTICLE INFO

## ABSTRACT

It is important and necessary to effectively detect the chemical warfare agents, such as highly toxic never agent sarin. However, based on the surface-enhanced Raman scattering (SERS) effect, detection of nerve agent simulant dimethyl methylphosphonate (DMMP) which is weakly interacted with SERS-active substrate has been the most challenge for the routine SERS detection method. To overcome this challenge, we put forward a thin water film confined SERS strategy. Under the space-confinement of water film, Raman measurements are carried out in the water evaporation process. The subsequent water evaporation induces concentrating of the DMMP molecules, which are thus successfully restricted within the strong electromagnetic field enhanced area above the SERS substrates, leading to the enhancement of their Raman signals. This study provides a new way to achieve the efficient SERS-based detection of the target molecules weakly interacted with the metal substrates.

* Corresponding authors. Fax: +86 551 65591434.
   E-mail addresses: duangt@issp.ac.cn (G. Duan), wpcai@issp.ac.cn (W. Cai).

## 1. Introduction

As a typical highly toxic nerve agent of chemical warfare agents, sarin is dramatically dangerous even at very low concentration. The rapid detection and identification of sarin is an important problem in national security that has attracted considerable attention for many years. As we known, surface-enhanced Raman scattering (SERS) spectroscopy is one of the most effective detection tools and offers some distinct advantages over other spectroscopic methods for homeland security applications. Due to its fingerprint characteristic, quick response and high sensitivity even to the single molecule-level [1–4], SERS spectroscopy has been widely applied in the fields of monitoring and detection of explosives, environmental pollutants, etc. [5–12]. However, there are few reports about the practical detection of such toxic molecules. The laboratory researches mainly use the structure similar but less toxic simulant molecule (e.g., dimethyl methylphosphonate used as sarin simulant).

For SERS detection technique, the target molecules need to stay at the strong electromagnetic field enhanced areas above the SERS substrates [13,14]. So ultrasensitive detection based on SERS effect has been traditionally restricted to molecules carrying functional groups with high affinity toward metal (gold or silver, etc.) surfaces. For the routine detection based on the SERS effect, it is a prerequisite for the substrate to capture or adsorb the analytes (or target molecules) within the strong field-enhanced areas. However, nerve agent simulant dimethyl methylphosphonate (DMMP) molecule has only weak interaction (or without good affinity) with the metal substrates which are highly SERS-active, and hence hardly adsorb on the substrates or have only very short residence time on them. In this case, it is very difficult to be detected by the SERS technique [15,16]. In addition, it is well known that DMMP molecule is a weak Raman scatterer with a very small cross-section on the order of $10^{-30}$ cm$^2$ sr$^{-1}$ molecule$^{-1}$ with 514.5 nm excitation for the strongest line [17], which further increased the difficulty of the detection. Thus, there are very limited reports on the enhanced Raman-based detection of DMMP and it is very difficult to realize the repeatable or quantitative measurements and trace detection [18–21]. At present, surface modification of the SERS substrates is often to be used to help capture analytes which have weak interaction with the metal surface [22,23]. It could lead to selective adsorption and enrichment of those molecules on the substrates. However, it is difficult to find the modifiers suitable for the specific target molecules, and to achieve the repeatable measurements and quantitative detection of them. In addition, for the organic modifiers, they would increase the Raman spectral complicacy and misidentification. How to effectively capture such molecules weakly interacted with the metal substrates, for the enhanced Raman-based monitoring and detection, is still a challenge.

Aiming at the existing problems, we first need to consider how to restrict the DMMP molecules within the effective field-enhanced area. Taking into account a big advantage of SERS detection is unaffected by water, and the evaporation rate of water is smaller than the volatilization rate of DMMP, we proposed a new strategy called thin water film confined surface-enhanced Raman scattering method to capture such hydrosoluble molecules, which are very weakly interacted with the metal substrates. That is, under the space-confinement of water film, Raman measurements are carried out in the water evaporation process. The subsequent solvent (water) evaporation induces concentrating of the target molecules and hence enhancing of the Raman signal. The details are reported in this article. It has been found that the SERS substrate can effectively capture the DMMP molecules by using the presented technique, and realized effective quantitative detection of DMMP aqueous solution. This study provides a new way to achieve the efficient enhanced Raman-based detection of the target molecules weakly interacted with the metal substrates.

## 2. Experimental

### 2.1. Preparation of SERS-active substrates

In this experiment, gold hierarchically micro/nanostructured bowl-like array was chosen as the SERS-active substrate. Its fabrication process was described in detail in our previous article [24]. Briefly, a 10-nm gold layer was pre-coated on an ITO conductive substrate. The pre-formed monolayer polystyrene (PS) colloidal crystal (2 μm in PS sphere-diameter) was then transferred onto the Au/ITO substrate. After heated at 110 °C for 5 min, the PS/Au/ITO substrate was used as a working electrode, and the electrodeposition was carried out in pure HAuCl$_4$ aqueous solution at −0.04 mA cm$^{-2}$ for 5 h at room temperature. Finally, the Au bowl-like array was obtained after dissolving the PS colloidal crystal in methylene chloride (CH$_2$Cl$_2$) and cleaning with deionized water for several times.

### 2.2. Characterization

The morphologies of the as-prepared substrates were observed on a field-emission scanning electron microscopy (FESEM, Sirion 200). The static water contact angles (CAs) of the substrates were measured on a contact angle meter SL200A (Solon Shanghai Co., Ltd.) at room temperature. The water droplet with 2 μL or 5 μL was used.

### 2.3. Raman spectral measurements

Firstly, $10^{-1}$ mol L$^{-1}$ DMMP aqueous solution was prepared by adding 216.5 μL DMMP liquid to 19.78 mL deionized water and stirring sufficiently. Then the solution was successively diluted to different concentrations with ten folds and stored in a refrigerator before use. A 20 μL DMMP aqueous solution, with a certain initial concentration, was dropped on the SERS substrates and spread out to form a thin water film with ∼3 mm in thickness (estimated by the droplet-volume and coverage area of the water film). The Raman spectra for the thin water film were thus collected after evaporation at room temperature for different time durations. The Raman measurements were carried out on a confocal microprobe Raman spectrometer (Renishaw inVia Reflex) with a laser beam of 632.8 nm in wavelength and 17 mW in total laser power. The laser beam was focused on the water film with ∼3 μm in spot size. All measurements were conducted at room temperature (∼20 °C) with the relative humidity ∼50%.

## 3. Results and discussion

### 3.1. Model of thin water film confined SERS strategy

Generally, in the traditional SERS-based detection process, the SERS-active substrates were firstly immersed in the solution containing the target molecules for a certain time to let the molecules adsorb on the metal substrate surfaces and then dried before spectral measurement. In the case that the target molecules are weakly interacted with the substrate, however, such procedures are usually invalid due to no or too few molecules adsorbed on the substrate after drying. The thin water film confined SERS strategy, we presented, which could overcome the above problem, is schematically illustrated in Fig. 1.

The target molecule aqueous solution is first dropped onto a SERS substrate with hydrophilic surface (Fig. 1a), and then spread
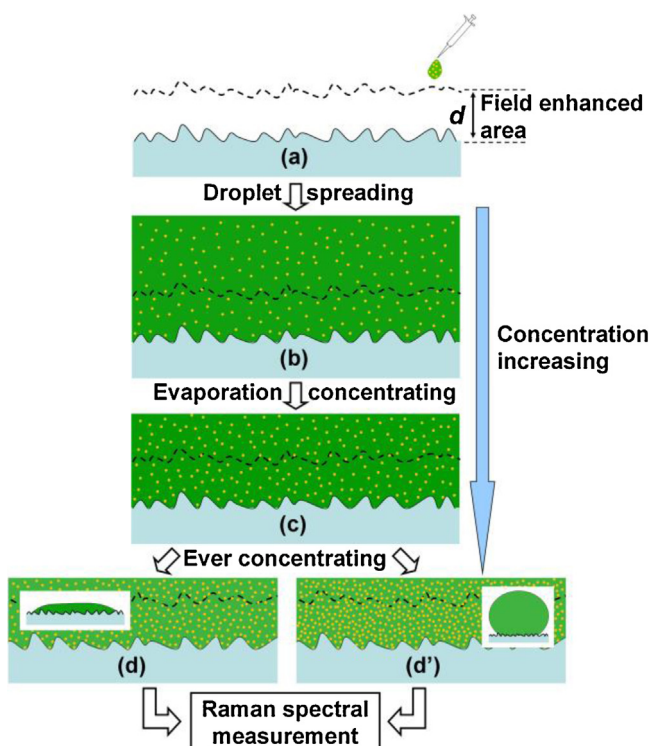
**Fig. 1.** Schematic illustration of the thin water film confined SERS strategy. (a) A clean SERS-active substrate. (b) An initial water film is formed after a certain amount of target solution is dropped on the substrate. (c) The water film is reduced in thickness and solute is concentrated due to the water evaporation. (d and d′) The water film thickness is comparable to that of the field-enhanced height for the hydrophilic and hydrophobic surface, respectively. The strongest thin water film confined SERS effect would be realized if Raman spectral measurements are conducted at this moment. The insets in the (d) and (d′) are the contact angle images showing hydrophilic and hydrophobic surfaces, respectively.

out to form a water film. The solute molecules (or the target molecules) are thus confined within the water film (see Fig. 1b). Assuming that the volatilization of the solute is ignored, the subsequent solvent evaporation induces the thinner and thinner water film, leading to continuous concentrating of the solutes in the film (see Fig. 1c). When the water film thickness is reduced to the nanometer level, the confined target molecules in the water film are all effectively localized within the space above the substrate where the electromagnetic field can be significantly enhanced during laser excitation (see Fig. 1d). If Raman spectral measurement is conducted at this moment, enhanced by both the concentrated solutes and the substrate surface, the Raman signal of the target molecules can reach the maximum.

In addition, if we defined an evaporation-induced concentrating-factor (CF) of the target molecules confined within the water film as the ratio of solute concentration in the water film at Raman spectral measurement stage to that at the initial stage, we can simply evaluate the concentration effect. Generally, compared with the evaporation of the solvent, volatilization of the molecules such as DMMP in solutions is relatively less, because of much heavier molecular weight, and the vapor tension of the water is more than 30 times higher than that of pure DMMP liquid at the temperature from 20 °C to 30 °C (the vapor tension of DMMP mentioned here come from the Material Safety Data Sheet of Sigma–Aldrich). Through semi-quantitatively evaluating the CF value, we can know the solvent evaporation-induced concentrating effect is quite significant. The details are described in Supplementary material Section I. For the enhanced substrates with hydrophobic surfaces, when the integrated water film is reduced to an enough thin thickness due to the evaporation, it could shrink horizontally and decrease the film coverage on the substrate, which further induces concentrating. So, the CF value should be higher in the local water films than that for the hydrophilic substrates, as shown in Fig. 1d′. In other word, the substrate with hydrophobic surface should be of better concentrating effect.

### 3.2. Detection of DMMP by thin water film confined SERS method

In recent years, we have synthesized many kinds of noble metal micro/nanostructured arrays as highly active SERS substrates [24–26]. Among them, gold hierarchically micro/nanostructured bowl-like array with a clean surface, which was fabricated by a simple electrochemical deposition method, is very suitable for the proposed thin water film confined SERS method. The fabrication process of Au bowl-like array was described in detail in the experimental section or our previous report [24]. Fig. 2a shows the typical morphology. The gold array consists of bowl-like pores, showing a hexagonally arranged pattern with 2-μm in period. The skeleton between the pores is built of a great deal of nearly vertical quasi-rod shaped nanoparticles. The static contact angle (CA) of such array's surface is ~105°, indicating the slightly hydrophobic surface (see Fig. 2b).
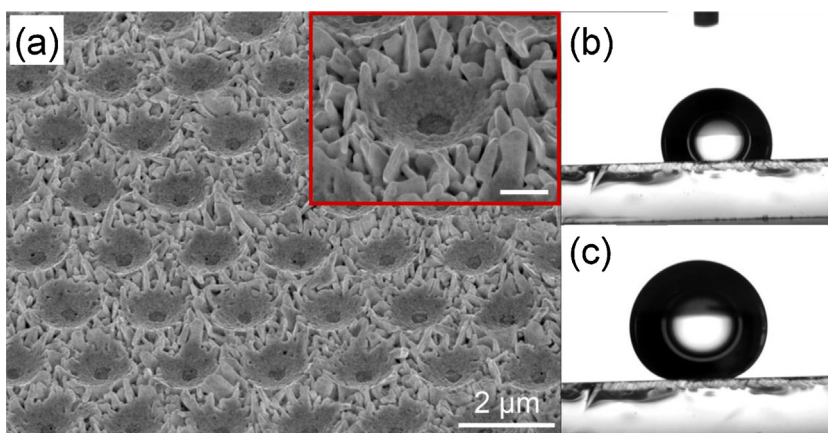


**Fig. 2.** The surface morphology and wettability of gold hierarchically micro/nanostructured bowl-like array. (a) FESEM image from tilted view. The inset: a local magnified image and the scale bar is 500 nm. (b and c) The water droplets' shapes on the array before and after surface modification with thiol, respectively. The volume of the water droplets is 2 μL and 5 μL respectively for (b) and (c).
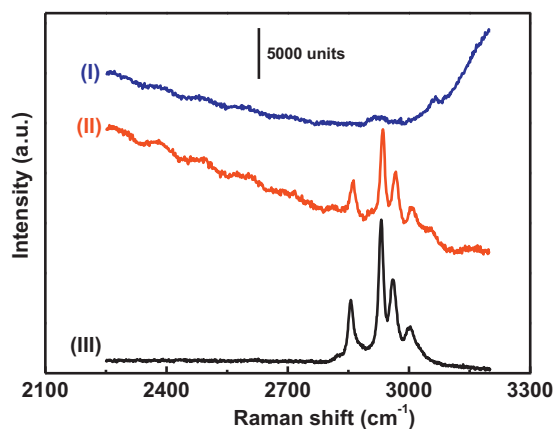
**Fig. 3.** Raman spectra of DMMP molecules. Curves (I) and (II) are for a droplet of $10^{-2}$ mol L$^{-1}$ DMMP aqueous solution on the SERS substrate after evaporation for a very short time and an optimized time, respectively. Curve (III) for pure DMMP liquid. Raman test conditions: 100% laser power, 10 s integration times, 1 acquisition.

When a droplet of DMMP aqueous solution, with 20 μL in volume and $10^{-2}$ mol L$^{-1}$ in initial concentration, was on the Au bowl-like array without surface modification, it spread out forming a water film with ∼3 mm in thickness. If the Raman measurement was conducted on such water film at the initial evaporation stage, no distinct signal could be detected except the background [see curve (I) in Fig. 3]. However, after evaporation for an enough long time before completely drying, as shown in Fig. 1d and d′, a significant Raman spectrum could be observed. The specific evaporation time was closely related with the ambient environment, such as temperature and relative humidity, etc. Under our experiment condition (∼20 °C room temperature and ∼50% relative humidity), if starting timing from when the distinct signals are very weak but detectable, after ∼300 s evaporation interval, we obtained the optimal Raman spectrum, as shown in curve (II) in Fig. 3. There are one dominant peak at 2936 cm$^{-1}$ and the other three smaller peaks at 2863 cm$^{-1}$, 2968 cm$^{-1}$ and 3006 cm$^{-1}$, respectively, which are in good agreement with the Raman spectrum of the pure DMMP liquid [as shown in curve (III) in Fig. 3] and other published literature [18]. These four main peaks in the higher wavenumber region are assigned to the C–H stretching modes of DMMP molecules [27]. In addition, there is another peak located in the lower wavenumber

region at 714 cm$^{-1}$ [see curve (I) of Fig. S1], is assigned to the P–C stretching mode of DMMP molecules [27]. However, through the same evaporation concentrating process on a non-SERS substrate (e.g., Si wafer substrate), no characteristic Raman signals of DMMP molecules were observed. In addition, we further performed some SERS measurements with pure DMMP liquid on gold substrates. After complete drying, we did not collect the characteristic Raman peaks of DMMP molecules, indicating no DMMP molecules would be left on the substrate while the water was completely evaporated. Obviously, these results demonstrated that DMMP molecules can be effectively detected by our proposed thin water film confined SERS method on a SERS-active substrate. That is, in order to realize the effective detection of DMMP molecules, not only the evaporation-induced concentrating effect, but also the highly active SERS substrate is necessary.

Further, the detailed Raman spectral evolution of the DMMP-contained water film on the Au bowl-like array substrate with the evaporation interval was recorded. Fig. 4a gives the spectra after evaporation for different durations for the same water film as that corresponding to curve (II) in Fig. 3. During initial stage of the evaporation, no characteristic Raman signals were detected and the film is opaque in the field of optical microscope, as shown in Fig. 4b. With the evaporation of solvent water, the water film gets thinner and thinner. When evaporation for $t_0$ duration, which varies from several minutes to few ten minutes, depending on the volume of solution droplet and the ambient conditions (temperature and relative humidity), the water film on the substrate was slightly transparent, and the characteristic peak at 2936 cm$^{-1}$ is very weak but detectable (see curve 1 in Fig. 4a). We start timing at this moment. The further evaporation leads to appearance of the other three characteristic peaks and continual enhancement of the four Raman peaks (see curves 2–6 in Fig. 4a). When the evaporation interval $\Delta t$ is upto ∼300 s, the intensity of the characteristic Raman peaks were increased to the maximum, as illustrated in curve 7 in Fig. 4a. The corresponding water film-photo is given in Fig. 4c, showing translucency or semi-transparence. The gold ordered arrangement pattern on the substrate looms up. After a little longer evaporation interval (∼20 s), the gold ordered array on the substrate is clearly appeared (Fig. 4d), corresponding to the complete evaporation or drying. Conducting Raman measurement at this moment, from curve 8 in Fig. 4a, we can see the weak peaks located at 2928 cm$^{-1}$ and 3060 cm$^{-1}$ are not the characteristic vibration peaks of the DMMP molecules, indicating that the
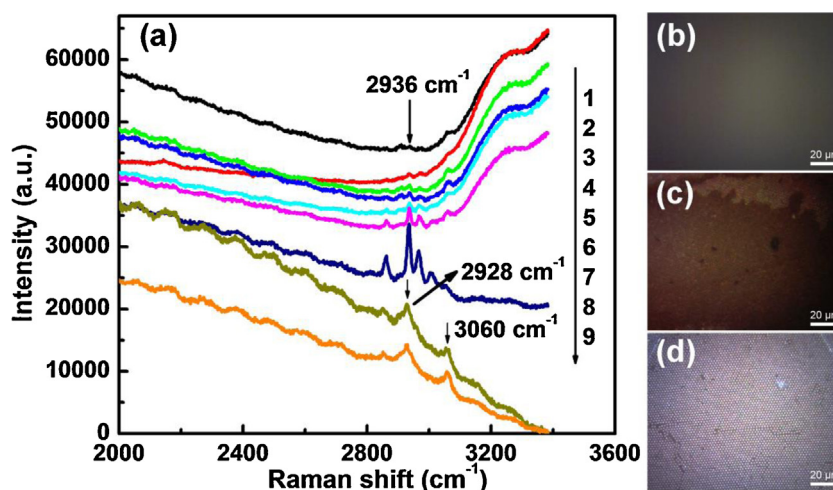


**Fig. 4.** Raman spectra and photos of the gold bowl-like array. (a) Raman spectra for a droplet of $10^{-2}$ mol L$^{-1}$ DMMP aqueous solution on the SERS substrate after evaporation for different intervals. Curves 1–9 correspond to the interval $\Delta t = 0$, 112 s, 155 s, 199 s, 243 s, 279 s, 301 s, 323 s and 348 s, respectively. (b–d) The photos of the gold bowl-like array covered with water film at the initial stage, optimized Raman-measured stage and completely dried stage, respectively. Raman test conditions: 100% laser power, 10 s integration times, 1 acquisition.
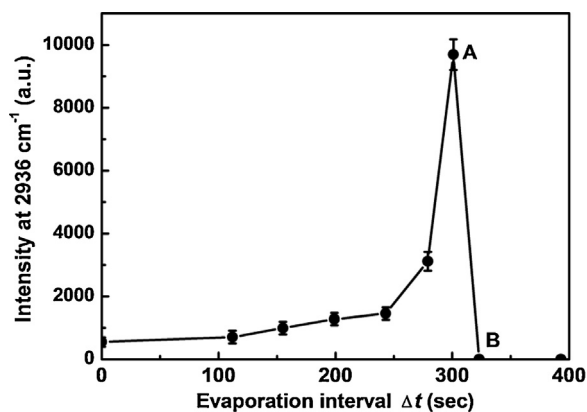
**Fig. 5.** Intensity of the Raman peak at 2936 cm$^{-1}$ versus evaporation interval (data from Fig. 4a). Point A: the maximal measured value. Point B: the peak vanishes.
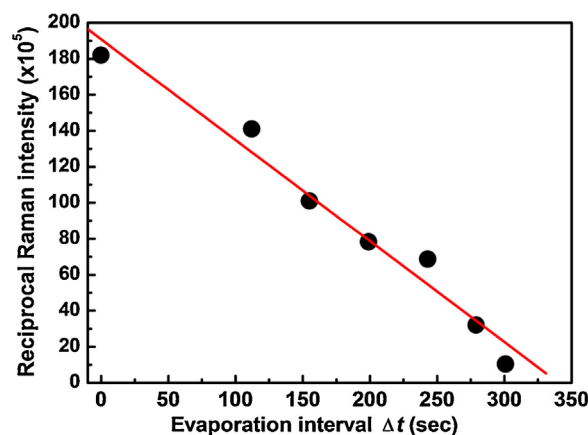


**Fig. 6.** Reciprocal Raman intensity at the peak 2936 cm$^{-1}$ versus evaporation interval (data from Fig. 5). The solid line is the linear fitting result.

longer evaporation induces the rapid decrease of the Raman peaks and finally vanishing. Representatively, Fig. 5 gives the intensity of the dominant peak at 2936 cm$^{-1}$ as a function of evaporation interval (the data from Fig. 4a), and clearly shows such evolution of the peak intensity.

The above successful observations of Raman characteristic peaks for the DMMP molecules in an aqueous solution are easily understood. This is mainly attributed to the thin water film confinement and subsequent evaporation-induced DMMP-concentrating within the space above the substrate where the electromagnetic field can be significantly enhanced during laser excitation, in addition to the local electromagnetic field enhancement of the gold micro/nanostructured array. Due to the space-confinement of the thin water film, evaporation of water leads to the concentrating of DMMP within a thinner and thinner film. In other words, by the water evaporation, more and more DMMP molecules in the film would be confined within the space with significant local electromagnetic field enhancement above the substrate, showing ever-increasing Raman signal with the evaporation interval, as demonstrated in Fig. 5. Obviously, after the water film is completely evaporated, the confinement effect thus disappears. In this case, DMMP molecules could not stay on the substrate and the corresponding Raman peaks vanish. It should be noted that the evaporation-induced reorientation of the DMMP molecules may also generate an additional Raman signal enhancement due to charge-coupling between the molecules and the metallic surface [16].

In order to further reveal the intensity-evolution of the Raman peaks with the evaporation interval shown in Fig. 5, we further semi-quantitatively analyzed the concentrating kinetics of DMMP molecules in the water film due to the evaporation, as detailed in Supplementary material Section II. We first put forward two assumptions, the solvent water evaporation rate is constant and the solute volatilization rate is proportional to the solution concentration. Through a series of derivation, we can find that the reciprocal solute concentration in the water film is nearly directly proportional to the evaporation time of water. When the solute concentration ($C$) in the water film is not enough high, or trace in amount, intensity ($I$) of its Raman-shift peaks should be directly proportional to $C$. In our case, DMMP is of good water-solubility and much larger molecule weight (124.08) [28]. So, Eq. (S6) could be a good description of the solute concentration evolution during water evaporation. From Eq. (S6′), the reciprocal intensity of the characteristic Raman peaks should be of nearly linear relation with the evaporation duration $t$ or evaporation interval $\Delta t$ of water, which has been confirmed by further spectral analysis. Fig. 6 gives the results corresponding to the reciprocal Raman intensity

at the peak 2936 cm$^{-1}$ versus the evaporation interval $\Delta t$ (data from Fig. 5), showing a good linear relation between them. This also implies that the volatile-loss could be very small or negligible during water film evaporation at ambient environment. By linear fitting, the plot in Fig. 6 can be described as

$$\frac{1}{I} = 190.88 - 0.56 \times \Delta t \qquad (1)$$

in which the intensity $I$ was multiplied by $10^{-5}$, and $\Delta t$ is in s.

### 3.3. Factors influencing thin water film confined SERS effect

The thin water film confined SERS effect mentioned above would be influenced by some factors, such as SERS-active substrates, evaporation conditions and volatility of the solute, etc. Obviously, the highly enhanced substrates, low solute's volatilization rate and appropriate solvent's evaporation rate would be beneficial to exhibiting significant thin water film confined SERS effect. In addition, further experiments have revealed that surface wettability of the substrate and the laser excitation power are also important to induce the strong thin water film confined SERS effect.

As mentioned before, the substrate with hydrophobic surface should be of stronger concentrating effect than that with hydrophilic surface. For confirmation, the parallel Au micro/nanostructured bowl-like array shown in Fig. 2a was first modified with thiol by immersion in an ethanol solution of 2 mM 1-hexadecanethiol for 2 h before rinsing with ethanol for several times and drying at room temperature, so that the substrate with more hydrophobic surface was obtained. After such modification, the static CA was increased from ~105° to ~160° (see Fig. 2c), exhibiting superhydrophobic surface. Using such modified array as SERS substrate, it has been found that the thin water film confined SERS effect is really significantly enhanced. Typically, Fig. 7 shows the SERS spectra of DMMP on the gold array with and without surface modification, measured after evaporation for an optimal duration, for the aqueous solution with initial concentration of 10$^{-3}$ mol L$^{-1}$. For the substrate without modification, the characteristic peaks of DMMP is very weak (see Fig. 7a). However, the surface modification induces much stronger Raman scattering peaks of DMMP (see Fig. 7b), and the intensity of the dominant peak at 2936 cm$^{-1}$ is one order of magnitude (~12 times) higher than that without modification. Comparing to the hydrophilic surface, the droplet on the superhydrophobic surface would shrink to a smaller one, the contact area between the droplet and the SERS substrate would gradually reduced, inducing the significant local concentration, leading more DMMP molecules reaching the effective field enhanced region. In a word, such Raman enhancement
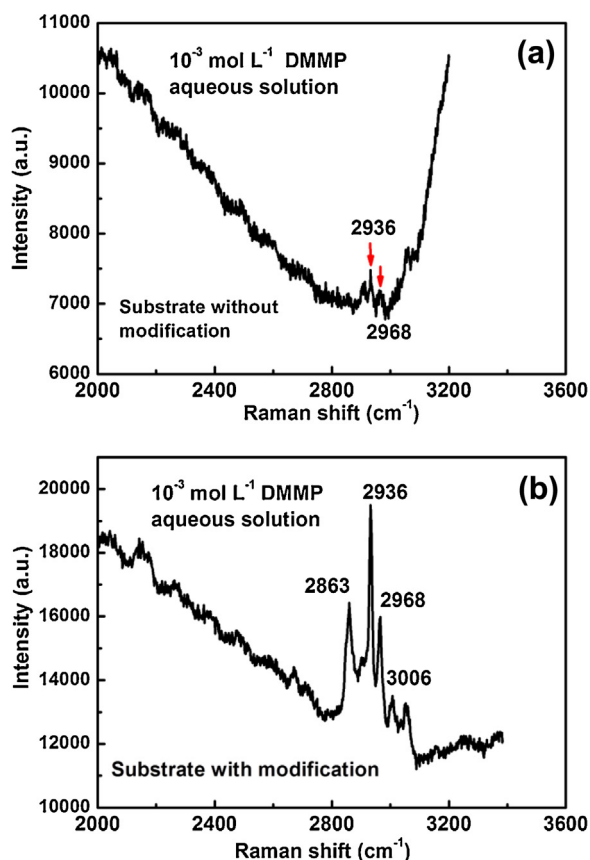
**Fig. 7.** Raman spectra of $10^{-3}$ mol L$^{-1}$ DMMP aqueous solution on the substrates without (a) and with (b) surface modification after optimal evaporation duration (see the text). Raman test conditions: 100% laser power, 5 s integration times, 1 acquisition.



**Fig. 8.** Laser power ($P$) dependence of the Raman spectra for the $10^{-2}$ mol L$^{-1}$ DMMP aqueous solution on the SERS-active substrate. (a) Raman spectra of DMMP aqueous solution droplet on the substrate, excited by different laser powers, after the evaporation for the same duration. The full excitation power of the equipment $P_{max} = 17$ mW. (b) The intensity of the peak at 2936 cm$^{-1}$ as a function of the laser excitation power. The solid-line is linear fitting result [data from (a)]. Raman text conditions: 10 s integration times, 1 acquisition.

could be attributed to the superhydrophobic surface-induced much higher CF value, leading to the stronger concentrating effect [5,29], in addition to the local electromagnetic field enhancement of the substrate.

We knew only when the thickness of the water film is reduced to the nanoscale by evaporation, can the concentrating effect and hence thin water film confined SERS effect reach maximum. However, for the measurements in the normal ambient conditions, the thickness of the water film, corresponding to the maximal measured Raman signals could be estimated to be in tens of micron scale (~8 μm to 30 μm in this study) based on the total evaporation duration to dry the water droplet on the substrate and its initial thickness. According to our experience, under the normal ambient conditions, the evaporation speed of the thin water film is ~μm/s in order of magnitude. It is too late to measure the Raman spectra when the water film is reduced to the nanoscale in thickness, because such thin water film would be completely evaporated or dried within one millisecond at the normal ambient environment. This is why the Raman peaks vanish immediately after the maximal measured value, as shown in Fig. 5 (points A and B). In other words, the maximal measured value is much smaller than the real maximal value. Although we can obtain CF of about $10^3$ in order of magnitude according to Eq. (S1′), the real maximal or optimal effect is far from reached, in the normal ambience.

Obviously, to further increase the thin water film confined SERS effect, we should decrease evaporation rate of the solvent water by some special ways, especially, since $t = t_0$ when the Raman shift peaks are weak but detectable (if the solute volatilization is neglectable relative to the evaporation of the solvent water). In fact, control of the evaporation rate needs some requirements and expe-
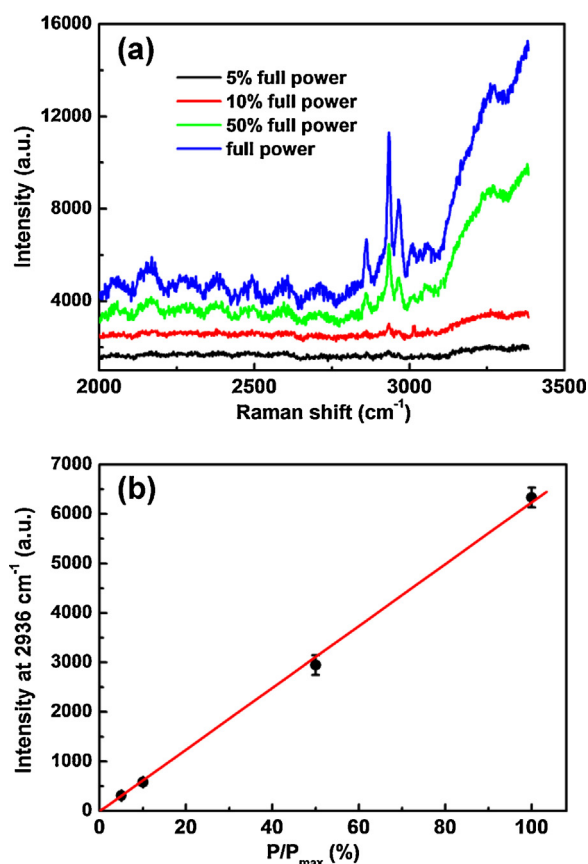
riences. At present, we try to control the evaporation rate by putting the substrate with the thinner water film (after evaporation for a certain time) into a quartz cell, which having a controllable opening to adjust the local humidity. Using this method, closing the opening when the ordered array was loomed up, as shown in Fig. 4c, we successfully collected the Raman signal of DMMP in the solution with $1 \times 10^{-4}$ mol L$^{-1}$ initial concentration, as shown in Fig. S2. If controlling the opening more skillfully, much lower initial concentration solution should be detected.

It is well known that the Raman scattering intensity of the target molecules is directly proportional to the laser excitation power. Using a higher laser power can lead to a stronger Raman scattering signal. But too high laser power will destroy the molecules due to the thermal effect, inducing the low Raman signal instead. However, our case is an exception. The thin water film could not only restrict the target molecules within a certain space but also protect them from the laser-induced damage since such water film can significantly reduce the laser-induced thermal effect. Fig. 8a shows a typical results corresponding to the Raman spectra of DMMP excited by different laser powers with the same evaporation time. The full power ($P_{max} = 17$ mW) of the equipment could be used in this study, while <5 mW is usually used in the conventional measurement. The intensity of the peak at 2936 cm$^{-1}$, shows very good linear relation with the power in the whole power range, as illustrated in Fig. 8b. The straight line passes through the origin. So, for our thin water film confinement and evaporation-concentrating strategy, we can use enough high laser excitation

power (>17 mW) to further increase Raman scattering intensity, exhibiting the stronger thin water film confined SERS effect.

Based on the above results, the thin water film can offer some functions: (i) confinement of the target molecules within the limited space above the SERS substrates. When the film is reduced to an enough thin thickness, the molecules are localized in the field-enhanced area though they are not adsorbed on the substrate. (ii) Concentrating of the target molecules. Evaporation of the solvent lead to concentrating of the solution, inducing concentrating of the target molecules in the film and increasing the number of the target-molecules in the field-enhanced area above the substrate. (iii) Reduction of laser-induced thermal effect. The thin water film can protect the target molecules from laser-induced damage. In this case, we can increase the laser excitation power to enhance the Raman signals.

## 4. Conclusion

We have presented a thin water film confined SERS method to effectively capture the hydrosoluble DMMP molecules within the strong electromagnetic field enhancement area above the SERS-active substrate surface and realized the effective quantitative detection of them. In this method, the DMMP molecules-contained aqueous solution with a certain initial concentration is dropped on the SERS substrate to form a thin water film on it. The DMMP molecules are thus restricted within it. Subsequent solvent (water) evaporation induces concentrating of the DMMP molecules within the space of strongly enhanced electromagnetic field above the substrate, and hence enhances the Raman signal. Herein, the thin water film can not only confine the DMMP molecules within a limited space, but also protect the DMMP molecules from laser-induced damage.

It should be mentioned that the hydrophobic substrate surface, slower evaporation and stronger excitation power can further enhance the thin water film confined SERS effect. Especially, the slow and controlled evaporation in the later stage would further lead to several orders of magnitude higher thin water film confined SERS effect. The strategy presented in this work could be a promising route for SERS-based detection of the soluble molecules, which are of small Raman scattering cross-section and hard to adsorb on the SERS substrate, by choosing appropriate solvents. Here, it should be noted that the strong volatile soluble molecules are not suitable for this strategy. In this case the liquid film can not confine these molecules.

## Acknowledgements

## Appendix A. Supplementary data

Supplementary data associated with this article can be found, in the online version, at http://dx.doi.org/10.1016/j.jhazmat.2015.10.022.

## References

[1] S. Nie, S.R. Emery, Probing single molecules and single nanoparticles by surface-enhanced Raman scattering, Science 275 (1997) 1102–1106.

[2] K. Kneipp, Y. Wang, H. Kneipp, L.T. Perelman, I. Itzkan, R. Dasari, M.S. Feld, Single molecule detection using surface-enhanced Raman scattering (SERS), Phys. Rev. Lett. 78 (1997) 1667–1670.

[3] T. Konishi, M. Kiguchi, M. Takase, F. Nagasawa, H. Nabika, K. Ikeda, K. Uosaki, K. Ueno, H. Misawa, K. Murakoshi, Single molecule dynamics at a mechanically controllable break junction in solution at room temperature, J. Am. Chem. Soc. 135 (2013) 1009–1014.

[4] J.H. Lee, J.M. Nam, K.S. Jeon, D.K. Lim, H. Kim, S. Kwon, H. Lee, Y.D. Suh, Tuning and maximizing the single-molecule surface-enhanced Raman scattering from DNA-tethered nanodumbbells, ACS Nano 6 (2012) 9574–9584.

[5] B.D. Piorek, S.J. Lee, M. Moskovits, C.D. Meinhart, Free-surface microfluidics/surface-enhanced Raman spectroscopy for real-time trace vapor detection of explosives, Anal. Chem. 84 (2012) 9700–9705.

[6] S. Botti, S. Almaviva, L. Cantarini, A. Palucci, A. Puiu, A. Rufoloni, Trace level detection and identification of nitro-based explosives by surface-enhanced Raman spectroscopy, J. Raman Spectrosc. 44 (2013) 463–468.

[7] H. Zhou, Z. Zhang, C. Jiang, G. Guan, K. Zhang, Q. Mei, R. Liu, S. Wang, Trinitrotoluene explosive lights up ultrahigh Raman scattering of nonresonant molecule on a top-closed silver nanotube array, Anal. Chem. 83 (2011) 6913–6917.

[8] P.R. Sajanlal, T. Pradeep, Functional hybrid nickel nanostructures as recyclable SERS substrates: detection of explosives and biowarfare agents, Nanoscale 4 (2012) 3427–3437.

[9] H. Tang, G. Meng, Q. Huang, Z. Zhang, Z. Huang, C. Zhu, Arrays of cone-shaped ZnO nanorods decorated with Ag nanoparticles as 3D surface-enhanced Raman scattering substrates for rapid detection of trace polychlorinated biphenyls, Adv. Funct. Mater. 22 (2012) 218–224.

[10] Q. An, P. Zhang, J. Li, W. Ma, J. Guo, J. Hu, C. Wang, Silver-coated magnetite-carbon core–shell microspheres as substrate-enhanced SERS probes for detection of trace persistent organic pollutants, Nanoscale 4 (2012) 5210–5216.

[11] G. Liu, W. Cai, L. Kong, G. Duan, Y. Li, J. Wang, Z. Cheng, Trace detection of cyanide based on SERS effect of Ag nanoplate-built hollow microsphere arrays, J. Hazard. Mater. 248 (2013) 435–441.

[12] M. Mueller, M. Tebbe, D.V. Andreeva, M. Karg, R.A. Alvarez Puebla, N. Pazos Perez, A. Fery, Large-area organization of pNIPAM-coated nanostars as SERS platforms for polycyclic aromatic hydrocarbons sensing in gas phase, Langmuir 28 (2012) 9168–9173.

[13] M. Moskovits, Surface-enhanced spectroscopy, Rev. Mod. Phys. 57 (1985) 783–826.

[14] S.J. Lee, A.R. Morrill, M. Moskovits, Hot spots in silver nanowire bundles for surface-enhanced Raman spectroscopy, J. Am. Chem. Soc. 128 (2006) 2200–2201.

[15] B. Sharma, R.R. Frontiera, A.I. Henry, E. Ringe, R.P. Van Duyne, SERS: materials, applications, and the future, Mater. Today 15 (2012) 16–25.

[16] R.A. Alvarez-Puebla, L.M. Liz-Marzan, Traps and cages for universal SERS detection, Chem. Soc. Rev. 41 (2012) 43–51.

[17] S.D. Christesen, Raman cross sections of chemical agents and simulants, Appl. Spectrosc. 42 (1988) 318–321.

[18] N. Taranenko, J.P. Alarie, D.L. Stokes, T. VoDinh, Surface-enhanced Raman detection of nerve agent simulant (DMMP and DIMP) vapor on electrochemically prepared silver oxide substrates, J. Raman Spectrosc. 27 (1996) 379–384.

[19] Y.H. Lee, S. Farquharson, Rapid chemical agent identification by surface-enhanced Raman spectroscopy, in: P.J. Gardner (Ed.), Chemical and Biological Sensing II, Proceedings of SPIE, Orlando, 2001, pp. 21–26.

[20] W.F. Pearman, A.W. Fountain, Classification of chemical and biological warfare agent simulants by surface-enhanced Raman spectroscopy and multivariate statistical techniques, Appl. Spectrosc. 60 (2006) 356–365.

[21] F. Yan, V.D. Tuan, Surface-enhanced Raman scattering detection of chemical and biological agents using a portable Raman integrated tunable sensor, Sens. Actuators B Chem. 121 (2007) 61–66.

[22] Z. Li, G. Meng, Q. Huang, C. Zhu, Z. Zhang, X. Li, Galvanic-cell-induced growth of Ag nanosheet-assembled structures as sensitive and reproducible SERS substrates, Chem. Eur. J. 18 (2012) 14948–14953.

[23] C. Zhu, G. Meng, Q. Huang, Z. Huang, Vertically aligned Ag nanoplate-assembled film as a sensitive and reproducible SERS substrate for the detection of PCB-77, J. Hazard. Mater. 211 (2012) 389–395.

[24] J. Wang, G. Duan, G. Liu, Y. Li, Z. Dai, H. Zhang, W. Cai, Gold quasi rod-shaped nanoparticle-built hierarchically micro/nanostructured pore array via clean electrodeposition on a colloidal monolayer and its structurally enhanced SERS performance, J. Mater. Chem. 21 (2011) 8816–8821.

[25] J. Wang, F. Zhou, G. Duan, Y. Li, G. Liu, F. Su, W. Cai, A controlled Ag–Au bimetallic nanoshelled microsphere array and its improved surface-enhanced Raman scattering effect, RSC Adv. 4 (2014) 8758–8763.

[26] J. Wang, G. Duan, Y. Li, G. Liu, Z. Dai, H. Zhang, W. Cai, An invisible template method towards gold regular arrays of nanoflowers by electrodeposition, Langmuir 29 (2013) 3512–3517.

[27] B.J. Van der Veken, M.A. Herman, Vibrational spectra of $CH_3PO(OCH_3)_2$ and isotopically substituted derivatives, Phosphorus Sulfur Relat. Elem. 10 (1981) 357–367.

[28] A.A. Tomchenko, G.P. Harmer, B.T. Marquis, Detection of chemical warfare agents using nanostructured metal oxide sensors, Sens. Actuators B Chem. 108 (2005) 41–55.

[29] V.L. Schmit, R. Martoglio, B. Scott, A.D. Strickland, K.T. Carron, Lab-on-a-bubble: synthesis, characterization, and evaluation of buoyant gold nanoparticle-coated silica spheres, J. Am. Chem. Soc. 134 (2011) 59–62.